Published in Sedimentary Geology v.219, pp. 196-207 (2009). © Elsevier Science Bv. DOI: 10.1016/j.sedgeo.2009.05.013

Relationships between hydrodynamic parameters and grain size in two contrasting transitional environments: the Lagoons of Venice and Cabras, Italy

Molinaroli E.[a], Guerzoni S.[b], De Falco G.[c], Sarretta A.[b], Cucco A.[c], Como S.[d], Simeone S.[d], Perilli A.[c], Magni P.[c]

[a]*Università Ca' Foscari Venezia, Dipartimento di Scienze Ambientali, Dorsoduro 2137, 30123 Venezia, Italy*

[b]*CNR - Istituto di Scienze Marine, Riva VII Martiri 1364/A, 30122 Venezia, Italy*

[c]*CNR - Istituto sull'Ambiente Marino, Loc. Sa Mardini, Torregrande-OR, Italy*

[d] *IMC - International Marine Center, Loc. Sa Mardini, Torregrande-OR, Italy*

Abstract

A comparison was made of shallow water sediments from the Lagoon of Venice (LV) and the Lagoon of Cabras (LC), comparing depositional environments and exploring the relationships between hydrodynamics and sedimentological parameters. The two water bodies are very different in size (LV: 360 km^2; LC: 22 km^2), and the sediments predominantly consist of silty-clay (LV: Mz ≈ 26 μm; LC: Mz ≈ 6 μm). However, there are large differences between the two lagoons with respect to sand (LV: mean 19%; LC: mean ~3 %) and clay (LV: mean 20%; LC: mean 45%) contents. The Lagoon of Venice (mean depth ~1 m) can be considered a tidal basin,

*Corresponding author. Tel. and fax: +39-041-2348583
E-mail address: molinaro@unive.it (Emanuela Molinaroli) stefano.guerzoni@ismar.cnr.it (Stefano Guerzoni) gianni.defalco@iamc.cnr.it. (Giovanni De Falco), alessandro.sarretta@ismar.cnr.it (Alessandro Sarretta), andrea.cucco@iamc.cnr.it (Andrea Cucco), s.como@imc-it.org (Serena Como), s.simeone@imc-it.org (Simone Simeone) angelo.perilli@iamc.cnr.it (Angelo Perilli), paolo.magni@iamc.cnr.it (Paolo Magni)

whereas the Lagoon of Cabras (mean depth ~2 m) has the character of a coastal lake in which wind is the main hydrodynamic forcing factor. A comparison of sediment grain-size distributions with water circulation patterns in different parts of the lagoons highlighted some interesting differences. Grain-size analyses of samples reveal a deficiency of particles around 8 μm in the LC, which is interpreted as reflecting the transition between cohesive flocs/aggregates and non-cohesive coarser silt particles, while the transition limit in the LV is ~ 20 μm. Thus, particles are cohesive below 8 μm in the LC and below ~20 μm in the LV. This is probably because of the differences in the clay/silt ratio, which is much lower in the LV (~ 0.3) than in LC (~1), conferring a "silt-dominated network structure" on most of the LV sediments.

The hydrographical data used were root mean square velocity (RMSV) and water residence time (WRT), computed under the main forcing conditions. The results show a general correlation between RMSV and sortable silt in the LC, and between RMSV and coarser sediments (63-105 μm) in the LV. Some significant differences between the lagoons were detected in the degree of correlation between WRT and grain size. Root mean square velocity (~7 cm s^{-1} in the LV and ~3 cm s^{-1} in the LC) was a greater forcing factor in the LC than in the LV. Conversely, WRT, which is on average ~16 days in the LV and ~19 days in the LC, has more influence in the LV. This study highlights the usefulness of comparing environments with different hydrodynamic energies, e.g., tidal and/or wind-driven currents, to elucidate and thereby improve our understanding of the processes governing the spatial distribution of sedimentological features, the transport mechanisms of sediments, and the relationship between them. The results demonstrate that the approach outlined in this study has the potential to provide a universal hydro-sedimentological classification scheme.

*Keywords***:** Hydrodynamic model; Root Mean Square Velocity; Water Residence Time; Grain size; Sortable silt.

1. Introduction

Links between hydrological and ecological processes in lagoonal environments have been assessed by many authors (e.g. Monsen et al., 2002). Hydrographical parameters such as water currents, water surface elevation and transport time-scales have been identified as fundamental parameters for the understanding of ecological processes. For example, hydrodynamic and sediment transport models can be used together with integrated models (e.g., CH3D, ADCIR) to address potential ecosystem responses to changes in specific conditions of interest (Teeter et al., 2001).

The hydrodynamics and sedimentology of the Lagoon of Venice (LV) have been extensively studied (Basu and Molinaroli, 1994; MAV-CVN, 1999; Umgiesser, 2000; Albani and Seranderei Barbero, 2001; Umgiesser et al., 2004a,b; Solidoro et al., 2004; Cucco and Umgiesser 2005, 2006), but rarely in the same context. Only recently have certain variables describing both the hydrodynamics and the transport time scales of the lagoon been compared with sediment distribution within the basin (Molinaroli et al., 2007). The Lagoon of Cabras (LC) has recently been investigated with respect to the spatial variability of bulk sediment properties (De Falco et al., 2004) and their relationships with macrofaunal communities (Magni et al., 2004, 2008a). Finally, hydrodynamic models have also been applied to the coastal Lagoon of Cabras (Ferrarin and Umgiesser, 2005).

Since the two lagoons are very different in size, hydrographical and sedimentological characteristics, and man-made forcing factors, the goal of the present paper is to shed light on the links between water circulation and sediment properties. Some fundamental variables describing both hydrodynamics and transport time-scales in the LV and LC were assessed using a numerical approach and compared with the bathymetry and sediment characteristics (including distribution) of the two basins. The approach chosen here to distinguish between the two lagoons has the potential to form the basis of a universal classification of such water bodies.

2. Sites

2.1. The Lagoon of Venice (LV)

The LV is the largest shallow coastal lagoon in the Mediterranean region (area: 550 km^2; extension: 50 km along the coast; width: 15 km) and is located in the northern Adriatic Sea along the north-eastern coast of Italy (45°N, 12°E) (Fig.1). The LV formed 6–7 kyr BP during the Flandrian transgression, when the rising sea flooded the Upper Adriatic Würmian paleoplain and delineated the coast in approximately the present position (Spencer et al., 2005a). Prior to the year 1500 AD, the rivers entering the Lagoon contributed approximately 700,000 m^3 of fine-grained material annually, most of which was deposited in salt marshes and mudflats; an additional 300,000 m^3 of sand entered from the sea to form tidal deltas.

A series of man-made changes affected the lagoon from the 15th to the 20th Centuries. These included diverting river flows away from the lagoon, opening and widening the tidal inlets, and creating waterways for navigation across the lagoon towards the inner, landward shore. The river diversions, construction of breakwaters at the lagoon inlets during the period 1808-1930, and increased dredging of lagoon channels for navigation purposes (shipping channels of up to 20 m deep were dredged in 1926 and 1970) have had a significant impact on the lagoonal morphology (Spencer et al. 2005b), and marine processes now prevail over natural lagoonal processes.

The lagoon is a complex combination of intertidal marshes, intertidal mudflats, submerged mudflats and navigation channels. Water exchange between the lagoon and the Northern Adriatic Sea is through the Lido, Malamocco and Chioggia inlets. Only 5% of the lagoon has a depth greater than 5 m, and 75% is less than 2 m, the average depth being 1.2 m. Two major wind regimes dominate in the region, the *Bora* from the north–east and the *Scirocco* from the south–east (maximum speeds ~ 50-60 km h^{-1}), occurring in spring and autumn respectively. The Adriatic tides, which locally reach mean ranges of 35 cm during neap tides and about 100 cm during spring tides, govern water exchange in the lagoon. Within the lagoon, these wind regimes generate strong circulation in addition to tidal flows, which is important for mixing and transport. They also create wind waves which are locally responsible for the resuspension of sediments in the shallow parts of the lagoon. (Umgiesser, 2000; Umgiesser et al., 2004a).

The average water volume is approximately 3.9 x 10^8 m^3, and the amount of salt water flowing in and out during each tidal cycle amounts to around one-third of the total volume of the lagoon

111 (Gačić et al., 2004). The terrestrial drainage basins discharging into the lagoon have a total area
112 of 1850 km^2 and provide an annual mean freshwater input of ~ 35 m^3 s^{-1}. The most important
113 streams are located in the northern basin, which receives on average more than 50% of the total
114 annual load. The associated sediment input was calculated at $33x10^3$ tons yr^{-1} for the years
115 1999/2000 (Collavini et al., 2005; Zonta et al., 2005). This hydrographical pattern creates a
116 typical brackish environment with a salinity gradient ranging from 10 PSU near the landward
117 shore to 32 PSU at the seaward inlets (Fig. 1). The subtidal areas of the lagoon are partially
118 vegetated by macroalgae and seagrasses (such as *Zostera marina, Z. noltii* and *Cymodocea*
119 *nodosa*).

120

121 **Insert Fig. 1.**

122

123 *2.2. The Lagoon of Cabras (LC)*

124 The LC is a shallow transitional system (mean depth ~1.7m, max. depth ~2.1m, Cannas et al.,
125 1998) located near the Gulf of Oristano on the west coast of Sardinia (Italy) in the western
126 Mediterranean Sea (39° 57'N, 08°29'E) (Fig. 2). With an area of 22 km^2, it is the largest brackish
127 basin on the island and one of the largest brackish systems of the western Mediterranean Sea. The
128 drainage basin discharging into the LC has a total area of 432 km^2 (Casula et al., 1999) and
129 includes two main streams, the *Riu Mare Foghe* and the *Riu Tanui*, located in the northern and
130 southern sectors of the lagoon respectively. The *Riu Tanui* has a much smaller catchment area
131 than the *Riu Mare Foghe*, but its sediment load is very important because of the intensive
132 agricultural activities in the area. In addition, the *Riu Tanui* used to discharge untreated urban
133 waste waters into the LC up to the year 2000 (Magni et al., 2008a).

134 Due to a low rainfall regime in the region (10 and 100 mm in July and December respectively)
135 (Pinna, 1989) and increasing demand for water, especially from agriculture, river discharge is
136 relatively limited. In the southern part of the basin, water exchange between the lagoon and the
137 adjacent Gulf of Oristano has been severely affected by a channel constructed in the late 1970s,
138 which can be closed by a dam to stop sea water flowing into the lagoon at high-tide (Fig. 2). An
139 additional connection to the adjacent Gulf of Oristano is via narrow, convoluted creeks which

140 flow into the main channel below the dam (Como et al., 2007). The artificial dammed channel
141 was constructed to prevent the flooding of villages situated around the lagoon by blocking the
142 tide and thereby avoiding inundation of the coastal areas at times of high river discharge which
143 would otherwise cause a rise in the lagoon's water level. Ironically, it has hardly ever been used
144 because since its construction fresh water inflow from the rivers has strongly decreased due to
145 increasing demand for water from land use. The dam favours the trapping of fine sediments
146 inside the lagoon. Tidal range is <25 cm, and exchange between the lagoon and the coastal
147 system is very limited. In contrast, tide- and wind-induced currents seem to cause sufficient
148 circulation of the internal water mass to bring about the resuspension and distribution of fine
149 sediment particles within the basin (De Falco et al., 2004).

150 Despite the current trend of increasing salinity caused by a progressive reduction of freshwater
151 input and increasing demand for water for land use (e.g., in agriculture), salinity can drop to <10
152 PSU following rainfall, rising to >30 PSU during dry periods (Magni et al., 2005).

153 The morphology of the southern part includes a complex system of dunes, the youngest line of
154 which faces the Gulf of Oristano. In contrast to the LV, the LC does not have morphological
155 features such as intertidal marshes, intertidal mudflats, submerged mudflats and navigation
156 channels.

157

158 **Insert Fig. 2.**

159

160

161 **3. Materials and methods**

162

163 *3.1. Sedimentological databases*

164

165 Lagoon of Venice (LV)

166 The samples processed in the present study are part of a database included in the MAV-CVN
167 (1999) study. Sediment samples from shallow lagoon beds (average depth ~1 m) were collected

168 at 70 sites during field work in 1997-1998, organised by the *Consorzio Venezia Nuova* (CVN)
169 and sponsored by the *Magistrato alle Acque* (Water Authority) (Fig. 1). At each site, the
170 sampling area consisted of a circle approximately 2 m across, with a central point fixed by
171 geographical co-ordinates. From each area, 6 sediment cores were taken (15 cm depth, 7 cm in
172 diameter, equally distributed within the circle) and combined to form a "composite" sample. In
173 this way, the probable sampling error was reduced by 60% (Krumbein, 1934).

174 After removing organic matter with H_2O_2, grain-size analysis of the sediments was performed by
175 dry sieving and hydrometer for sand (>63 μm) and mud (<63 μm) fractions respectively. The
176 sample treatment and analytical details have been described elsewhere (Molinaroli et al., 2007).
177 The silt-clay boundary was taken to be 4 μm.

178

179 Lagoon of Cabras (LC)

180 The samples processed in this study were collected during April-May 2001. Thirty stations,
181 spaced 750 m apart, were selected on a regular square grid covering the whole lagoon (Fig. 2).
182 Sediment samples were collected using a manual corer (40 cm long, 10 cm diameter) penetrating
183 ~20 cm into the sediments.

184 The samples were treated with H_2O_2 in order to eliminate organic matter and wet sieved through
185 a 63 μm mesh. The sand fraction (>63 μm) was treated with 1-0N HCL to dissolve the $CaCO_3$ of
186 any bioclastic material, which was occasionally present in significant quantities due to colonies
187 of *Ficopomatus enigmaticus*. The bioclastic component can significantly affect grain size
188 distribution, leading to a misleading interpretation of the relationships between grain size data
189 and hydrodynamics. Grain-size analysis of the <63 μm fraction was performed using a Galai CIS
190 1 laser particle sizer (Molinaroli et al., 2000). The sample treatment and analytical details have
191 been described elsewhere (De Falco et al., 2004).

192 Sediments were classified using the textural classification of gravel-free muddy sediments on
193 ternary diagrams proposed by Flemming (2000). Again, the silt-clay boundary was taken to be 4
194 μm.

195 The two sets of grain-size data were analysed in different ways. The LV dataset is based on a
196 sedimentation technique while the LC dataset is based on the time-of-transition technique.

197 The problem of comparing grain-size analyses based on different techniques is not a minor issue
198 and has been discussed by several authors (Konert and Vanderbergen, 1997; McCave et al., 2006;
199 Goossens, 2008). Konert and Vandenberg (1997) indicate that an 8 μm laser corresponds to 2 μm
200 settling on sediments of fluvial, aeolian and lacustrine origin. McCave et al. (2006) showed that
201 the laser sizer increasingly overestimates the sortable silt (10-63 μm) fraction as the fine silt/clay
202 content measured by Sedigraph rises, and the differences between laser and Sedigraph become
203 negligible when the 10-63 μm fraction is higher than 40%. Molinaroli et al. (2000) found a
204 correspondence between < 4 μm (Galai) and < 2 μm (Sedigraph), with less accentuated
205 differences using the time-of-transition laser technique (Galai) than laser diffraction (Malvern).
206 In any case, the results provided by the two techniques cannot be directly used for objective
207 comparison unless some normalisation procedures are applied (Goossens, 2008). To achieve this,
208 we analysed 30 samples with both techniques and the relationships between the data obtained
209 were estimated by means of variation/residuals analysis and regression analysis. Galai was found
210 to overestimate the coarse-silt fraction (22-63 μm) only slightly (~3%) and the finest fraction (< 1
211 μm) more considerably (~8%), whilst fine silt and clay were slightly underestimated (2-5%).
212 Contrary to Goossens, we found a good correspondence between hydrometer and Galai for the <8
213 μm and <22 μm fractions. The equations were:

214 % Galai = 1.055 x % Hydrometer ($r=0.75$; $p<0.001$) for the < 22 μm fraction, and
215 % Galai = 1.035 x % Hydrometer ($r=0.82$; $p<0.001$) for the < 8 μm fraction.
216 The equation was then used to recalculate the numerical results from the hydrometer to allow
217 comparison with the results from the Galai particle sizer. The data obtained from the conversion
218 show slight differences of ±2% with respect to the original LV dataset (range 1-4%).
219 In any case, the bias of the laser may actually have reduced the apparent differences between the
220 two data sets and therefore our main conclusions are valid.

221 TOC content was measured for the total sample set in both LV and LC sediments.

222

223 *3.2. Hydrographical parameters*

224

225 The hydrology of the LV and LC was investigated by means of a 2D hydrodynamic numerical
226 model based on the finite element method. The model resolves the vertically integrated shallow
227 water equations in their formulations with water levels and transport on a numerical domain
228 represented by a staggered finite element grid. Details of the equations and of the numerical
229 treatment adopted by the model are given in Umgiesser and Bergamasco, (1995), Umgiesser et al.
230 (2004a) and Cucco and Umgiesser (2005). The model has been successfully applied in other
231 studies to reproduce wind- and tide-induced water circulation in the LV (Umgiesser et al., 2004b,
232 Solidoro et al., 2004 and Cucco and Umgiesser, 2005) and LC (Ferrarin and Umgiesser, 2005,
233 Magni et al., 2008b). In order to reproduce and analyse the general water circulation and flushing
234 features of the two basins, numerical simulations based on local meteo-marine forcing factors
235 were carried out.

236 Specifically, for the LV, the tide can be considered as the main forcing factor affecting water
237 circulation. Even during strong wind events, such as the Bora and the Scirocco winds (from the
238 south-east and north-east respectively), their influence on water circulation is mostly negligible in
239 comparison to daily tidal forcing effects (Gačić et al., 2002, Cucco and Umgiesser, 2005).

240 By contrast, in the LC, water circulation is mainly influenced by the wind. The main wind regime
241 in the area, and therefore the main factor affecting water circulation in the LC, is the Mistral
242 wind, a strong wind blowing from the north-west (Ferrarin and Umgiesser, 2005, Magni et al.,
243 2008b). With an average water displacement of less than 40 cm, the tides in this basin are very
244 weak but are still considered to be the main factor promoting exchange between the Oristano
245 Gulf and the lagoon.

246 Therefore, in order to reproduce the general water circulation and flushing features of the two
247 basins in the LC, both the wind and tidal effects have to be considered. Simulations were carried
248 out on separate numerical domains representing the LV and the LC. The water circulation and
249 flushing features of the LV were analysed when only the tide was forcing the basin, whereas both
250 the Mistral wind and the tide were considered for the LC. We refer the reader to Cucco and
251 Umgiesser (2005) and Ferrarin and Umgiesser (2005) for a detailed description of the numerical
252 grids, model parameterization and boundary conditions adopted in this study.

253 In order to compare the hydrographical and flushing features of the two lagoons, the root mean
254 square current velocities (RMSVs) and water residence times (WRTs) were calculated from the

model results. The RMSV was computed for each element of the two numerical domains using the formula:

$$RMSV(x,y) = \sqrt{\overline{vel(x,y)}^2}$$

where *vel(x, y)* is the horizontal velocity at point (*x,y*), the bar indicating a suitable average.

The RMSV gives a good estimate of hydrodynamic activity in the two basins. Specifically, the erosion process is generally dependent on bottom shear stress (WBSS), of which the formula is:

$$WBSS = \rho \cdot C_B \cdot RMSV^2$$

where C_B is the bottom drag coefficient and ρ is the water density.

In both the LV and LC, the sediment samples are characterized by very low depth variability, less than 8% for the LC and 10% for the LV, whereas they are characterized by high variability in terms of RMSV values (see section 4). The WBSS variability within each dataset is largely governed by RMSV variability, which can be properly used as a parameter to characterise the variability of hydrographical forcing factors in each basin (Molinaroli et al., 2007).

Wind wave dynamics and their influence on hydrology and sediment transport were not considered in this study, for either lagoon. In the LV, waves induced by strong Bora and Sirocco winds can cause wave heights of up to 50 cm in the shallow lagoon areas (Ferrarin, et al. 2008), where they can be considered an important factor in the sediment resuspension process. Nevertheless, since the tide is the main factor forcing water circulation, tidal currents were assumed to be the main factor controlling long term sediment transport and distribution inside the LV, rather than wind wave forcing. In the LC, where wind fetch is strongly restricted by the limited size of the basin, waves induced by strong wind events are characterized by very low amplitude, and their effects on sediment dynamics are comparable to the effects of the main current flow.

The WRTs of the two lagoons were computed following an Eulerian approach. The WRT was defined as the time required for each element of the domain to replace most of the mass of a conservative tracer with new water. It was calculated with reference to the mathematical expression given by Takeoka (1984a, b), known as the remnant function. A detailed description of the method adopted to compute it may be found in Umgiesser et al. (2004b) and in Cucco and

283 Umgiesser (2006). WRT gives additional information – with respect to the RMSV – on the
284 hydrographical features of the two basins. For example, concerning the flushing time of water
285 within a selected area of a basin, WRT is necessary to identify areas where water masses tend to
286 stay at rest, which is not necessarily dependent on water current velocity alone. Indeed, the
287 presence of closed circulation cells tends to promote water trapping even when such
288 hydrographical features are characterised by high current velocity, especially along the edges
289 (Cucco and Umgiesser, 2006). Furthermore, computation of WRTs makes it possible to identify
290 areas characterised by similar RMSV values but which are more heavily influenced by the
291 dynamics of either the open sea or the innermost parts of the lagoon.

292

293 **4. Results and discussion**

294

295 *4.1. Sedimentological comparison of LV and LC*

296 A comparison of the two lagoons highlights the main differences in both morphological-
297 sedimentological and hydrodynamic characteristics (Tab.1).

298

299 **Insert Tab. 1**

300

301 The sediments of the LV and LC are mostly silty-clayey (mean mud content ~80% and 90% of
302 dry weight respectively). However, as evident from Table 1, there are large differences between
303 the two lagoons with respect to the contents of sand (LV: mean 19%, min. 1, max. 90; LC: mean
304 3%, min. 0, max. 17) and clay (LV: mean 20%, min. 3, max. 38; LC: mean 45%, min. 29, max.
305 58). Overall, silt is the dominant size fraction in the LV (61% on average), whereas silt and clay
306 both account for 45% on average in the LC (Tab. 1). The LV thus has a lower clay/silt ratio
307 (mean 0.3) than the LC (mean 0.9). The clay/silt ratio, particularly with non-cohesive silts
308 (sortable silts), seems to be related to hydrodynamic conditions, as will be discussed later.

309 Sediment TOC is much lower in the LV (mean 1.1%; min. 0.3; max. 3.1) that in the LC (mean
310 3.3%; min. 1.0; max. 4.3). TOC in marine sediments is normally associated with the finest grain-

size fraction and for this reason organic carbon content is commonly compared on the basis of mud content (Tyson, 1995). However, this does not take into account the fact that the mud fraction may contain both non-cohesive (sortable) silts and cohesive muds, the former (like sand) containing little organic carbon. The spatial variability of TOC in the LC – despite the uniformly muddy nature of the sediment – can indeed be better explained in terms of its association with the cohesive mud fraction. In the LV, by contrast, the situation is exactly the opposite, the sediment being dominated by non-cohesive silt which, as a consequence, has lower organic carbon content.

The LV sediments were classified in terms of the influence of marine processes, and three groups were identified, containing samples from: (a) the northern part and near the landward shore, (b) the central area, (c) the southern part and near the three seaward inlets. In terms of physical energy, the lagoon varies from relatively high energy on the seaward side, which is influenced by tidal flows through the three main inlets connecting the lagoon to the Adriatic, to quiescent conditions on the landward side.

The averaged frequency curves of samples from the (a) and (b) groups show that the mud fractions are composed of two distinct populations (Fig. 3). The (a) group includes very well sorted coarser silts with a pronounced peak at about 63 μm, indicating an affinity to very fine sand, and a second population consisting of poorly sorted finer silts and clays with one peak at about 11 μm and a second at 1.5 μm. The (b) group also includes very well sorted coarser silts with a pronounced peak at about 63 μm, and a second population consisting of poorly sorted finer silts and clays with modest peaks. An important characteristic is that in both (a) and (b) groups the two populations are separated by a deficiency of particles at about ~22 μm, which means that they are both composed of two major sub-populations, one greater and one smaller than this size.

Insert Fig. 3.

The averaged frequency curve of the LC samples shows that the mud fraction is composed of two distinct populations (Fig. 4). One includes well sorted silt with a peak at ~11 μm (medium silt), the other poorly sorted finer silt and clay with a well-defined peak at ~4 μm and a smaller peak at ~1.5 μm. An important feature is that the mud fraction is characterised by a deficiency of

340 particles at ~8 μm, which means that they are composed of two major sub-populations, one
341 greater and one smaller than this size. The 8 μm size fraction marks the transition between the
342 sortable coarser-grained and the aggregated finer-grained sub-populations (McCave et al., 1995).
343 A similar observation was made by Chang et al. (2006, 2007) who observed a lack of particles at
344 ~8 μm in a back-barrier tidal basin in the Wadden Sea.

345

346 **Insert Fig. 4**

347

348 The textural composition of the LV and LC sediments in terms of sand/silt/clay ratios is shown
349 on a ternary diagram (Fig. 5), the location of the data points within the diagram reflecting specific
350 hydrodynamic energy conditions (Flemming, 2000).

351 The diagram reveals that the sediments of the three LV groups plot in a belt reflecting an
352 intermediate energy gradient (Flemming, 2000). The textural gradient of group (a) shows a
353 progressive shift towards lower silt/clay content (i.e., towards the clay apex), indicating a rapid
354 fall in energy.

355 The sediments in group (b) are richer in silt and sand fraction, corresponding to the energy
356 conditions of mudflats. The sediments of the last group (c) are composed mainly of sand and silt
357 fractions, corresponding to energy conditions usually associated with sand flats and mixed flats
358 (Flemming, 2000).

359 From a geological point of view, the distribution of the surficial sediments bears the imprint of
360 past fluvial inputs and their reworking as a result of the lagoon's hydrodynamics. It is possible to
361 distinguish three main basins: a northern basin, characterized by the presence of deposits from the
362 rivers Piave and Sile, a southern basin, characterized by sedimentation of inputs from the rivers
363 Brenta and Bacchiglione, and a central basin with river Brenta sediments reworked by the
364 lagoon's hydrodynamics. Mineralogically speaking, there are differences between the northern
365 sector of the lagoon, where carbonate-rich sediments prevail, and the silicate-rich southern sector.
366 Clayey minerals are more abundant in low energy areas of the lagoon, particularly on the
367 landward side (Molinaroli and Rampazzo, 1987; Bonardi et al., 2004).

Almost all the samples from the LC have high mud contents (clay/silt ratio ~ 1), corresponding to energy conditions usually associated with mature mudflats. Petrographically speaking, the samples consist of clayey silts and silty clays (Fig. 5). The sediments originate mainly from volcanic rocks with high clay mineral contents (Barca et al., 2005).

The different textural properties of the sediments in the two lagoons indicate different hydrodynamic processes and hence different depositional conditions. The presence of finer materials in the LC reflects a generally lower-energy hydrodynamic regime, although similar sedimentary features were also observed in the northern part and near the landward shore of the LV, indicating that the prevailing hydrodynamic conditions in the LV are similar to those in the LC.

Van Ledden and co-workers (2004) showed that mud content as a descriptor for the transition between non-cohesive and cohesive erosion behaviour was more accurate than clay content. Specifically, those authors considered both the "cohesion" and the "network structure" of sediments, and set the transition between non-cohesive and cohesive mixtures at 5-10% clay (< 4 μm) content (see Figs. 2 and 5 in van Ledden et al., 2004). Thus a combination of textural classification (Flemming, 2000) and structural attributes was suggested. In this scheme, all the LC sediments can be classified as "cohesive clay-dominated", whilst the LV sediments are "partly cohesive clay-dominated", but mostly with a "cohesive silt-dominated network structure"

Insert Fig. 5

4.2. Characterisation of the mud fraction in the LV and LC

The grain-size composition of the mud in the two lagoons was investigated in more detail. The dynamic behaviour of fine particles (<63 μm) in the course of transport is quite different and more complicated than that of sand. This is because fine-grained sediments are generally composed of two different particle groups with different hydraulic properties – non-cohesive silts (well-sorted coarser silt) and cohesive mud (unsorted silty clays) (Dyer, 1986; Soulsby and Whitehouse, 1997). Flocculation is affected by many factors, including suspended sediment concentrations (SSC), turbulence-induced shear stress, differential settling of flocs, and sticky

organic matter in the water column (Dyer and Manning, 1999; Geyeret al., 2004). The individual contribution of these factors to floc size is unclear (Xu et al., 2008).

In the ternary plot in Fig. 6, the fine-grained sediment fraction is represented by the <8 μm and the 8–63 μm fractions. The under 8–10 μm fraction is the non-sortable mud fraction (cf. McCave et al., 1995; Chang et al., 2006, 2007), mainly consisting of aggregated or flocculated particles composed of small mineral grains and organic matter, whereas the 8–63 μm fraction predominantly consists of non-aggregated, silt-sized mineral grains. Because the former particle group (<8-10 μm) is subject to flocculation and aggregation during transport and deposition, whereas the latter (>8-10 μm in size) tends to be transported in the form of single mineral grains (McCave et al., 1995), an attempt was made to differentiate between cohesive and non-cohesive sediments in the two lagoons. In the LC, the <8 μm grain size fraction was found to correlate most strongly with TOC and organic matter content (De Falco et al., 2004; Magni et al., 2008a). This fraction, associated with reduced hydrodynamics and low water exchange (Magni et al., 2008b), was also found to correlate with increased risk of hypoxic/anoxic conditions, sulphide development and massive death of benthos and fish (Magni et al., 2005). Following McCave et al. (1995) and Chang et al. (2006, 2007), we lumped all particles <8 μm into a cohesive mud fraction (Fig. 6). The resulting ternary plot shows that most of the samples from the LV are composed of coarser sediment than the samples from the LC, which are mainly composed of silty clay (<8 μm). Generally speaking, coarser non-cohesive silts reflect stronger near-bed flows and selective deposition. The location of LV sediments changes only slightly in the new ternary diagram (cfr. Fig. 5 and 6). The position of the LC samples, by contrast, changes considerably, most of the samples shifting towards the <8 μm apex (Fig. 6).

Insert Fig. 6.

To investigate trends in the sediments of the two lagoons when the cut-off for the cohesive fraction was raised even higher, we plotted the <22 μm fraction against the 22–63 μm and >63 μm fractions (Fig.7).

425 The location of the LV sediments in the plot now shows most of the samples from the northern
426 lagoon having shifted towards the <22 μm apex. The rest of the sediments in the LV, however,
427 are still mainly composed of non-cohesive particles. In contrast, the cohesive fraction prevails in
428 all LC sediments.

429 The 22 μm limit is used here to distinguish between 'coarse' and 'fine' mud fractions in the
430 distribution. This boundary roughly separates the fine particles included in aggregates (inherited,
431 geochemically flocculated or biologically agglomeratated) from non-aggregated particles during
432 sedimentation.

433 The transition from non-cohesive to cohesive behaviour can be seen as occurring at 8 μm and 22
434 μm for the LC and LV respectively. The cohesive behaviour of the coarser fraction in the LV is
435 probably due to the role of the silt-dominated network structure, as highlighted by Van Ledden et
436 al. (2004), in a context of very low clay/silt ratios (~0,3), as is the case with the LV sediments.

437 In other words, all the LC sediments can be classified as “cohesive clay-dominated”, whilst the
438 LV sediments are “partly cohesive clay-dominated”, but mostly with a “cohesive silt-dominated
439 network structure” that shifts the transition from non-cohesive to cohesive behaviour from 8 μm
440 to 22 μm.

441

442 **Insert Fig. 7.**

443

444 *4.3. Hydrographical comparison of the LV and LC*

445 RMSV and WRT values were computed for the LV and LC and their distribution patterns
446 compared. In the case of the LV, the hydrodynamic pattern determined by the tides is highly
447 complex due to the presence of channels, tidal marshes and islands. Water entering and exiting
448 the four sub-basins through the three seaward inlets generates strong currents in the main
449 channels. The four sub-basins have different sizes and therefore different circulation patterns. A
450 detailed description of the general water circulation in the basins has been made by Umgiesser
451 (2000) and is therefore not repeated here. Important to note here, however, is that the average
452 RMSV for the LV as a whole is about 15 cm s^{-1} with a standard deviation of about 20 cm s^{-1},
453 which indicates high spatial heterogeneity. For example, the highest RMSV values are found in

454 the main channels and in the inlets, where they reach ~60 cm s^{-1}. On the other hand, in the
455 innermost regions, along parts of the watersheds between sub-basins and along the landward
456 shore, RMSV values fall to <6 cm s^{-1}. Table 1 only lists RMSV values corresponding to the
457 shallow parts of the LV, where the range is between 0 and 18 cm s^{-1} and the mean ~7 cm s^{-1},
458 whereas Fig. 8 shows RMSV patterns for the whole lagoon.

459

460 **Insert Fig. 8.**

461

462 As with the RMSVs, WRTs in the LV are heterogeneously distributed over the sub-basins, with a
463 mean of 16 days and a standard deviation of about ± 7 days. WRT values range from less than 1
464 day close to the inlets to 26 days in the innermost areas. The spatial distribution is mainly
465 dependent on the relative distance from the three seaward inlets and the location of the main
466 channels (Fig. 9).

467

468 **Insert Fig. 9.**

469

470 In the LV, RMSV is inversely related to WRT, the latter being lowest in the vicinity of the inlets
471 and the channels where tidal flushing is more efficient, and highest in the innermost areas and
472 along the three lagoonal watersheds, where the weak tidal flow replaces the waters very slowly.
473 A full description of the model's results can be found in Cucco and Umgiesser (2006).

474 In the case of the LC, the circulation pattern is completely different to that of the LV, being
475 characterised by the presence of cyclonic and anti-cyclonic eddy structures promoted mainly by
476 the interaction of the Mistral wind with the tide. A large cyclonic vortex dominates the
477 hydrodynamics of the central and northern parts of the lagoon, and two smaller vortices
478 characterise the residual circulation in the southern part. Tidal action promotes weak exchanges
479 through the main inlet, which accordingly do not generate strong currents within the lagoon. The
480 pattern of both RMSV and WRT is therefore mainly influenced by wind-induced current
481 circulation. A detailed description of the general water circulation in the LC has been made by

Ferrarin and Umgiesser (2005) and is thus not repeated here. More recently, Magni et al (2008b) proposed a number of scenarios characterized by different hydraulic balances between the Gulf of Oristano and the Cabras Lagoon, and carried out numerical simulations to predict the evolution of both hydrographical and ecological variables within the system under different meteorological forcing conditions.

The average RMSV in the LC was found to be 3 cm s^{-1} and the standard deviation 2 cm s^{-1}. Higher values were found along the edges of the vortices and along the lagoonal shores, and lower values in the central part of the lagoon and in the cores of the vortices. The maximum RMSV, 49 cm s^{-1}, was computed for the western shore of the central part of the basin. An intensification of the RMSV was also detected in the southern part of the basin along the eastern shore where a maximum value of 31 cm s^{-1} was computed (Fig.10).

Insert Fig. 10.

As in the case of the LV, WRT in the LC is inversely related to RMSV, varying from 24 days in the central part of the lagoon to a few hours near the river mouths and the network of channels connecting the basin with the main inlet. The mean value is ~19 days with a low standard deviation (5 days). As with RMSV, the spatial distribution of WRT is strongly influenced by the wind-induced circulation pattern. Higher WRTs are found in the core regions of the circulation vortices, and lower values are found along the edges of the vortices and the shores of the lagoon (Fig. 11).

Insert Fig. 11.

Comparison of RMSV and WRT patterns in the LV and LC reveals striking differences, despite the two parameters being inversely correlated in both cases. The LV has highly variable hydrodynamic activity and flushing features. Strong current velocity and high flushing capacity are found in the main channels, in the seaward inlets and nearby areas, whereas weak water circulation and flushing capacity are detected in shallow areas, and in the northern and landward

parts of the lagoon. The variability in hydrodynamic activity in the LV is thus mainly dependent on the presence and location of the channels and on the relative distance from the inlets.

In the LC, by contrast, hydrodynamic activity and flushing features are evenly distributed over the basin and the water renewal capacity of the tidal action is very weak. Higher current velocities and flushing capacity are detected in the shallow areas along the shores of the lagoon, whereas lower RMSVs and higher WRTs are found in the deeper, central parts of the lagoon. The LC is therefore comparable to a lake, in which exchanges are mainly promoted by river inputs and by evaporation and precipitation processes. Here, the water circulation is mainly caused by wind action, which generates strong currents along the shores and weak currents in the deeper parts.

A final observation is that the two basins are characterized by different water circulation patterns, which can be considered the main reason for their different sedimentological features.

4.4. Hydro-sedimentological correlation in the LV and LC

As we have seen, there are substantial differences between the two lagoons in terms of both sedimentological and hydrographical characteristics. With this data at hand, we made an attempt to expand the ternary diagram of Flemming (2000) by adding the hydrodynamic conditions defined by the RMSVs and WRTs in the two contrasting lagoons. In this more complex system, we associate variations in RMSV and WRT values in the LV with sortable silt/aggregates ratios, and variations in RMSV values with sand/mud ratios. In the LC, we associate variations in RMSV and WRT values with sortable silt/aggregate ratios (Fig. 12).

In the LC, RMSV shows a good positive correlation with the 63-8 μm grain-size fraction (Fig. 12a) and a reasonable negative correlation with the <8 μm grain-size fraction (Fig. 12b).

In the LV, RMSV shows a good positive correlation with the 105-63 μm grain-size fraction (Fig. 12c) and a negative correlation with the <22 μm grain-size fraction (Fig. 12d), corresponding to very fine sand and non-cohesive coarser silt respectively. Furthermore, we found good correlations between the <22 μm grain-size fraction and WRT for those samples located outside the regression confidence band in the plot (Fig. 12e). These samples are from areas which, despite having similar RMSV values, are more heavily influenced by the dynamics of either the

open sea or the innermost parts of the lagoon. This result in the LV data confirms the findings of Molinaroli et al. (2007), which showed a high correlation between the <31μm grain size fraction and WRT.

The relationship between grain size and hydrographical parameters underlines the differences between the two lagoons, in which the mud fractions are composed of different populations (finer in the LC and coarser in the LV) affected by different hydrodynamics.

Insert Fig. 12.

5. Conclusions

The main conclusions of the detailed comparison of hydrographical and grain-size data from the Lagoon of Venice (LV) and the Lagoon of Cabras (LC) are the following:

1. The sediments of the LV and LC mostly consist of silty clay (mean mud content ~80% and 90% respectively).
2. The ternary diagrams show that most of the sediments from the LC are composed of cohesive silt (<8 μm), whereas the sediments from the LV are mainly composed of a coarser population 8-63 μm in size, the cut-off for the silty fraction being ~20 μm.
3. The LV is characterised by high variability of both hydrodynamic activity and flushing features. This variability in the lagoon is mainly dependent on the presence and location of the channels and on the relative distance from the seaward inlets.
4. In the case of the LC, both hydrodynamic activity and flushing features are roughly uniform over the basin. Therefore, the LC is more comparable to a lake, in which exchanges are promoted mainly by river inputs and by evaporation and precipitation, and where water circulation is mainly wind-driven.

5. A positive correlation was found between RMSV and the non-cohesive (8-63 μm) and fine sand (63-105 μm) fractions in the LC and LV respectively.
6. Current velocity (RMSV) determines the variability of the cohesive grain-size fraction in both lagoons, whilst residence time (WRT) is important only in the LV, where circulation cells tend to promote water trapping.
7. The approach chosen here to distinguish between the two lagoons could potentially form the basis of a universal classification system for such water bodies.

Acknowledgements

This work was funded by the SIGLA project (Sistema per il Monitoraggio e la Gestione di Lagune ed Ambiente) of the Italian Ministry for Scientific Research.

We would like to thank the Water Management Authority of Venice for providing data. Mr. George Metcalf revised the English text. We thank the anonymous reviewers and the Editor for their careful reviews and comments.

584 **References**

585 Albani, A.D., Serandrei Barbero, R., 2001. The distribution of surface sediments in the lagoon of
586 Venice (Italy) in the 1980s. Atti Istituto Veneto di Scienze, Lettere ed Arti, Venice, 159, 363-
587 378.

588 Barca, S., Carmignani, L., Oggiano, G., Pertusati, P.C., Salvadori, I., 2005. Geological map of
589 Sardinia. Scale 1:200,000. Edited by Comitato Regionale per il Coordinamento della
590 Cartografia Geologica e Geotematica della Sardegna. Co-ordinator L. Carmignani.

591 Basu, A., Molinaroli, E., 1994. Toxic metals in Venice lagoon sediments: model, observation,
592 and possible removal. Environmental Geology 24, 203-216.

593 Bonardi, M., Tosi, L., Pizzetto, F., 20004. Mineralogical characterization of the Venice Lagoon
594 top sediments. In: Campostrini, P. (Ed.), CORILA Research Programme 2001-2003 Results,
595 vol. II, pp. 145-155.

596 Cannas, A., Cataudella, S., Rossi, R., 1998. Gli stagni della Sardegna. C.I.R.S.PE. Centro Italiano
597 Ricerche e Studi sulla Pesca.

598 Casula, R., Coni, M., Diliberto, L., Murrau, A., 1999. Comparison between experimental and
599 theoretical assessment of phosphorous and nitrogen loadings flowing into a coastal lagoon. In:
600 Brebbia, C.A., Anagnostopoulos, P. (Eds.). Proceedings Water Pollution V. Lemnos, Greece.
601 WIT Press, Southampton, UK, pp. 341-351.

602 Chang, T.S., Joerdel, O., Flemming, B.W., Bartholomä, A., 2006. Importance of flocs and
603 aggregates in muddy sediment dynamics and seasonal sediment turnover in a back-barrier tidal
604 basin of the East Frisian Wadden Sea (southern North Sea). Marine Geology 235, 49-61.

605 Chang, T.S., Flemming, B.W., Bartholomä, A., 2007. Distinction between sortable silts and
606 aggregated particles in muddy intertidal sediments of the southern North Sea. In: Flemming,
607 B.W., Hartmann, D. (Eds.). From particle size to sediment dynamics. Sedimentary Geology
608 (Spec. Issue) 202, 453-463.

609 Como, S., Magni, P., Casu, D., Floris, A., Giordani, G., Natale, S., Fenzi, G.A., Signa, G., De
610 Falco, G., 2007. Sediment characteristics and macrofauna distribution along a human-modified
611 inlet in the Gulf of Oristano (Sardinia, Italy). Marine Pollution Bulletin 54, 733-744.

612 Collavini, F., Bettiol, C., Zaggia, L., Zonta, R., 2005. Pollutant loads from the drainage basin to
613 the Venice Lagoon (Italy). Env. Int, 31 (7), 939-947.

614 Cucco, A., Umgiesser, G., 2005. Modeling the tide induced water exchanges between the Venice
615 Lagoon and the Adriatic Sea. Scientific Research and Safeguarding of Venice. Proceedings of
616 the Annual Meeting of the Corila Research Program, 2003 Results, 3, 385-402.

617 Cucco, A., Umgiesser, G., 2006. Modeling the Venice Lagoon water residence time. Ecological
618 Modelling 193, 34-51.

619 De Falco, G., Magni, P., Teräsvuori, L.M.H., Matteucci, G., 2004. Sediment grain-size and
620 organic carbon distribution in the Cabras lagoon (Sardinia, west Mediterranean). Chemistry
621 and Ecology 20, (Supplement 1), S367-S377.

622 Dyer, K.R., 1986. Coastal and Estuarine Sediment Dynamics, John Wiley, Chichester, UK.

623 Dyer, K.R., Manning, A.J., 1999. Observation of the size, settling velocity and effective density
624 of flocs, and their fractal dimensions. Journal of Sea Research 41, 87-95.

625 Ferrarin, C., Umgiesser, G., Cucco, A., Hsu, T.W., Roland, A., Amos, C. L., 2008. Development
626 and validation of a finite element morphological model for shallow water basins. Coastal
627 Engineering. 55, (9), 716-731

628 Ferrarin, C., Umgiesser, G., 2005. Hydrodynamic modelling of a coastal lagoon: The Cabras
629 lagoon in Sardinia, Italy. Ecological Modeling 188, 340-357.

630 Flemming, B.W., 2000. A revised textural classification of gravel-free muddy sediments on the
631 basis of ternary diagrams. Cont. Shelf Res. 20, 1125–1137.

632 Gačić, M., Kovacevic, V., Mazzoldi, A., Paduan, J., Arena, F., Mosquera, I. M., Gelsi, G., Arcari,
633 G., 2002. Measuring water exchange between the Venetian Lagoon and the open sea. EOS,
634 Transactions, AGU 83, (20), 217:221 222.

635 Gačić, M., Mazzoldi, A., Kovacevic, V., Mancero Mosquera, I., Cardin, V., Arena, F., Gelsi, G.,
636 2004. Temporal variations of water flow between the Venetian lagoon and the open sea. Journal
637 of Marine System, 1, 33-47.

638 Geyer, W.R., Hill, Kineke, P.S., 2004. The transport, transformation and dispersal of sediment by
639 buoyant coastal flows. Continental Shelf Research 24, 927-949.

640 Goossens, D., 2008. Techniques to measure grain-size distributions of loamy sediments: a
641 comparative study of ten instruments for wet analysis. Sedimentology 55, 65-96

642 Konert, M., Vandenberghe, J., 1997. Comparison of laser grain size analysis with pipette and
643 sieve analysis: a solution for the underestimation of the clay fraction. Sedimentology 44,
644 523–535.

645 Krumbein, W.C., 1934. The probable error of sampling for mechanical analysis. American
646 Journal of Science 27: 204-214.

647 Magni, P., Micheletti, S., Casu, D., Floris, A., De Falco, G., Castelli, A., 2004. Macrofaunal
648 community structure and distribution in a muddy coastal lagoon. Chemistry and Ecology,
649 20(S1): S397-S407.

650 Magni, P., Micheletti, S., Casu, D., Floris, A., Giordani, G., Petrov, A., De Falco, G., Castelli, A.,
651 2005. Relationships between chemical characteristics of sediments and macrofaunal
652 communities in the Cabras lagoon (Western Mediterranean, Italy). Hydrobiologia 550, 105-
653 119.

654 Magni P., De Falco, G., Como, S., Casu, D., Floris, A., Petrov, A.N., Castelli, A., Perilli, A.,
655 2008a. Distribution and ecological relevance of fine sediments in organic-enriched lagoons:
656 the case study of the Cabras lagoon (Sardinia, Italy). Marine Pollution Bulletin, 56: 549-564.

657 Magni P., Como, S., Cucco, A., De Falco, G., Domenici, P., Ghezzo, M., Lefrançois, C.,
658 Simeone, S., Perilli, A., 2008b. A multidisciplinary and ecosystemic approach in the Oristano
659 Lagoon-Gulf system (Sardinia, Italy) as a tool in management plans. Transitional Water
660 Bulletin, 2(2): 41-62. Available on line: http://siba2.unile.it/ese/issues/55/xxx/twb
661 08v2n2p41.pdf

662 MAV-CVN, 1999. Mappatura dell'inquinamento dei fondali lagunari. Studi ed indagini, relazione
663 finale luglio 1999. Consorzio Venezia Nuova., Venice, Italy.

664 McCave, I.N., Manighetti, B., Robinson, S.G., 1995. Sortable silt and fine sediment
665 size/composition slicing: parameters for palaeocurrent speed and palaeoceanography.
666 Paleoceanography 10, 593–610.

667 McCave, I.N. Hall, I.R., Bianchi, G. G., 2006 Laser vs. settling velocity differences in silt
668 grainsize measurements: estimation of palaeocurrent vigour. Sedimentology 53, 919-928.

669 Molinaroli, E., Rampazzo, G., 1986. Contributo alla conoscenza mineralogica dei sedimenti
670 superficiali della Laguna Veneta: i minerali pesanti. *Atti e Memorie*, Accademia Patavina,
671 part.II, XCVII, 159-176.

672 Molinaroli, E., De Falco, G., Rabitti, S., Portaro, R.A., 2000. Stream-scanning laser system,
673 electric sensing counter and settling grain-size analysis: a comparison using reference
674 materials and marine sediments. Sedimentary Geology 130, (3-4), 269-281.

675 Molinaroli, E., Guerzoni, S., Sarretta, A., Cucco, A., Umgiesser, G., 2007. Link between
676 hydrology and sedimentology in the Lagoon of Venice, Italy. Journal of Marine System 68,
677 303-317.

678 Monsen, N.E., Cloern, J.E., Lucas, L.V., 2002. A comment on the use of flushing time, residence
679 time, and age as transport time scales. Limnol. Oceanog. 47, 1545-1553.

680 Pinna, M., 1989. Il clima in Provincia di Oristano (ed.), La Provincia di Oristano: il territorio la
681 natura e l'uomo. Pizzi Spa, Milano, 38-48.

682 Solidoro, C., Melaku Canu, D., Cucco, A. and Umgiesser, G., 2004. A partition of the Venice
683 Lagoon based on physical properties and analysis of general circulation. Journal of Marine
684 System 51, 147-160.

685 Soulsby, R.L, Whitehouse, R., 1997. Threshold of sediment motion in coastal environments. Proc
686 Pacific Coasts and Ports Conf 1, University of Canterbury, Christchurch, New Zealand, pp.
687 149-154

688 Spencer, T., Da Mosto, J., Fletcher, C.A., 2005a. Introduction: geological and environmental
689 context. In: Fletcher, C.A., Spencer, T., (Eds.), Flooding and Environmental Challenges for
690 Venice and its Lagoon: State of Knowledge. Cambridge University Press, Cambridge, UK,
691 pp. 17-19.

692 Spencer, T., Fletcher, C.A., Da Mosto, J., 2005b. Introduction: physical processes, sediments and
693 morphology of the Lagoon of Venice. In: Fletcher, C.A., Spencer, T., (Eds.), Flooding and
694 Environmental Challenges for Venice and its Lagoon: State of Knowledge. Cambridge
695 University Press, Cambridge, UK, pp. 355-357.

696 Takeoka, H., 1984a. Exchange and transport time scales in the Seto Inland Sea. Continental Shelf
697 Research 3 (4), 327-341.

698 Takeoka, H., 1984b. Fundamental concepts of exchange and transport time scales in a coastal sea.
699 Continental Shelf Research 3 (3), 311-326.

700 Tyson, R. V. (1995). Sedimentary organic matter. Chapman & Hall, London.

701 Teeter, A.M., Johnson, B.H., Berger, C., Stelling, G., Scheffner, N.W., Garcia, M.H., Parchure,
702 T.M., 2001. Hydrodynamic and sediment transport modeling with emphasis on shallow-water,
703 vegetated areas (lakes, reservoirs, estuaries and lagoons). In: Best, E.P.H., Barko, J.W., (Eds.),
704 Modelling Sediment Resuspension,Water Quality and Submerged Aquatic Vegetation.
705 Hydrobiologia, 444, pp. 1-23.

706 Umgiesser, G., 2000. Modeling residual currents in the Venice Lagoon. In: Yanagi, T., (Ed.),
707 Interactions between Estuaries, Coastal Seas and Shelf Seas. Terra Scientific Publishing
708 Company (TERRAPUB), Tokyo, Japan, pp. 107 124.

709 Umgiesser, G., Bergamasco, A., 1995. Outline of a primitive equation finite element model.
710 Istituto Veneto di Scienze, Lettere ed Arti, Venice, Italy, 12, 291-320.

711 Umgiesser, G., Sclavo, M., Carniel, S. and Bergamasco, A., 2004a. Exploring the bottom stress
712 variability in the Venice Lagoon. Journal of Marine System 51, 161-178.

713 Umgiesser, G., Melaku Canu, D., Cucco, A. and Solidoro, C., 2004b. A finite element model for
714 the lagoon of Venice, Italy. Development and calibration. Journal of Marine System 51, 123-
715 145.

716 Van Ledden, M., van Kesteren, W.G.M., Winterwerp, J.C., 2004. A conceptual framework fort
717 he erosion behaviour of sand-mud mixtures. Continental Shelf Research 24, 1-11.

718 Xu, F., Wang, D-P., Riemer, N., 2008. Modeling flocculation processes of fine-grained particles
719 using a size resolved method: comparison with published laboratory experiments. Continental
720 Shelf Research 28, 2668-2677.

721 Zonta, R., Collavini, F., Zaggia, L., Zuliani, A., 2005. The effect of floods on the transport of
722 suspended sediments and contaminants: A case study from the estuary of the Dese River
723 (Venice Lagoon, Italy). Environmental International 31 (7): 948-958.

724

725 TABLES

726 Table 1. Mean values of sedimentary, hydrological and environmental variables of the two
727 lagoons.

728

729 **FIGURE CAPTIONS**

730

731 Fig. 1. Lagoon of Venice. Location of sediment sampling sites. Dotted areas: seagrass beds. ○ =
732 samples from northern part and near landward shore, × = samples from central area; Δ =
733 samples from southern part and near three seaward inlets.

734 Fig. 2. Lagoon of Cabras. Location of sediment sampling sites.

735 Fig. 3. Average frequency distribution curve of mud samples in LV dataset; solid line = LV (a)
736 samples from northern part and near landward shore; dashed line = LV (b) samples from
737 central area.

738 Fig. 4. Average frequency distribution curve of mud samples in LC dataset.

739 Fig. 5. Ternary diagram of surficial LV and LC sediments based on sand/silt/clay ratios with cut-
740 off between clay and silt set at 4 μm. Boundary lines define different sediment types as in
741 Flemming (2000). ● = LC sediment samples; ○ = LV (a) samples from northern part and
742 near landward shore, × = LV (b) samples from central area; Δ = LV (c) samples from
743 southern part and near three seaward inlets.

744 Fig. 6. Ternary diagram of surficial LV and LC sediments showing sand/sortable silt/aggregate
745 ratios with cut-off between aggregated (cohesive) particles and sortable silt set at 8 μm. ● =
746 LC sediment samples; ○ = LV (a) samples from northern part and near landward shore, × =
747 LV (b) samples from central area, Δ = LV (c) samples from southern part and near three
748 seaward inlets.

749 Fig. 7. Ternary diagram of surficial LV and LC sediments based on sand/sortable silt /aggregate
750 ratios with cut-off between aggregated (cohesive) particles and sortable silt set at 22 μm. ●
751 = LC sediment samples; ○ = LV (a) samples from northern part and near landward shore, ×
752 = LV (b) samples from central area, Δ = LV (c) samples from southern part and near three
753 seaward inlets.

754 Fig. 8. Distribution of RMSVs (cm s^{-1}) in the Lagoon of Venice (from Molinaroli et al. 2007).

755 Fig. 9. Distribution of WRTs (days) in the Lagoon of Venice (from Molinaroli et al. 2007).

756 Fig. 10. Distribution of RMSVs (cm s^{-1}) in the Lagoon of Cabras.

757 Fig. 11. Distribution of WRTs (days) in the Lagoon of Cabras.

758 Fig. 12. Ternary diagrams of surficial sediments from LC (left) and LV (right) based on ratios of
759 sand/sortable silt (63–8 μm)/aggregates (<8 μm) and sand/sortable silt (63–22
760 μm)/aggregates (<22 μm) respectively, and bivariant plots showing correlations between
761 grain-size fractions and hydrographical parameters. ○ = LV samples from northern part
762 and near landward shore, × = LV samples from central area, Δ = LV samples from
763 southern part and near three inlets. Arrows in the ternary diagrams indicate increasing
764 weight of hydrographical parameters.

Table 1

Table 1. Mean values of sedimentary, hydrological and environmental variables of the two lagoons.

Lagoon of Venice	**Mean**	**Median**	**sd**	**Min**	**Max**
Surface (Km^2)	360				
Depth (m)	1	1	0.5	0.2	2.9
Sand (%)	19	6	26	1	90
Silt (%)	61	67	20	6	83
Clay (%)	20	20	9	3	38
Mz (μm)	26	26	4	19	39
Clay/Silt	0.3	0.3	0.1	0.1	0.7
Non-cohesive/Cohesive	0.7	0.7	0.3	0.2	1.6
RMSV ($cm\ s^{-1}$)	7.1	6.7	3.3	0.1	17.8
WRT (days)	16	16	7	0	26.0
TOC (%)	1.1	1	0.6	0.3	3.1
Lagoon of Cabras	**Mean**	**Median**	**sd**	**Min**	**Max**
Surface (km^2)	22				
Depth (m)	1.7	1.8	0.2	1.2	2.1
Sand	3	0	5	0	17
Silt	50	49	7	30	65
Clay	45	46	6	29	58
Mz (μm)	6	4.4	6.5	3	38
Clay/Silt	0.9	0.9	0.2	0.5	1.4
Non-cohesive/Cohesive	0.3	0.2	0.1	0.1	0.9
RMSV ($cm\ s^{-1}$)	4.4	3.8	2.6	1.2	12.2
WRT (days)	19	20	5	0.5	24
TOC(%)	3.3	3.4	0.7	1	4.3

Figure 1

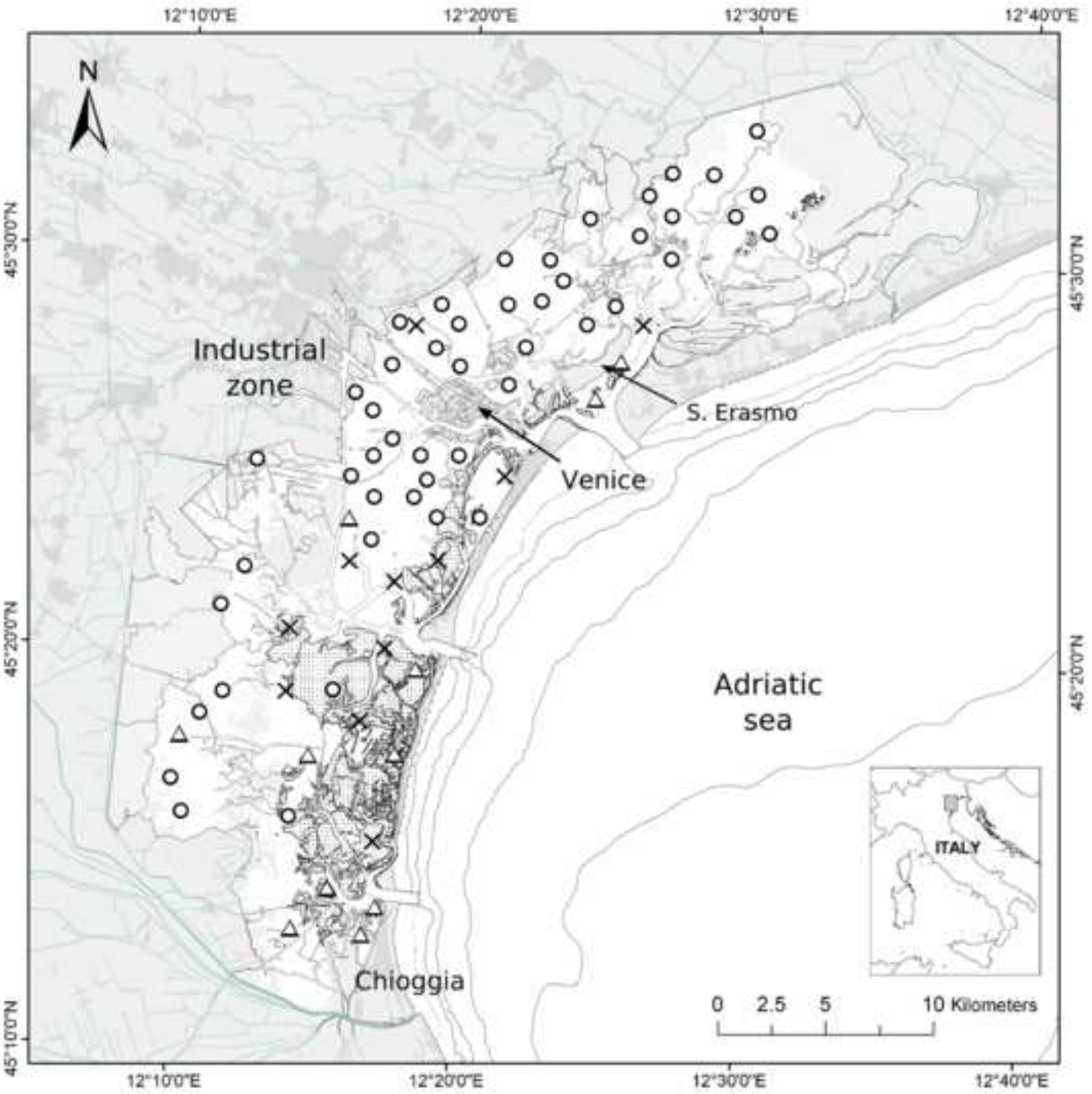
12°10'0"E
12°20'0"E
12°30'0"E
12°40'0"E
N
45°30'0"N
45°20'0"N
45°10'0"N
Industrial zone
S. Erasmo
Venice
Adriatic sea
Chioggia
ITALY
0 2.5 5 10 Kilometers

Figure 23

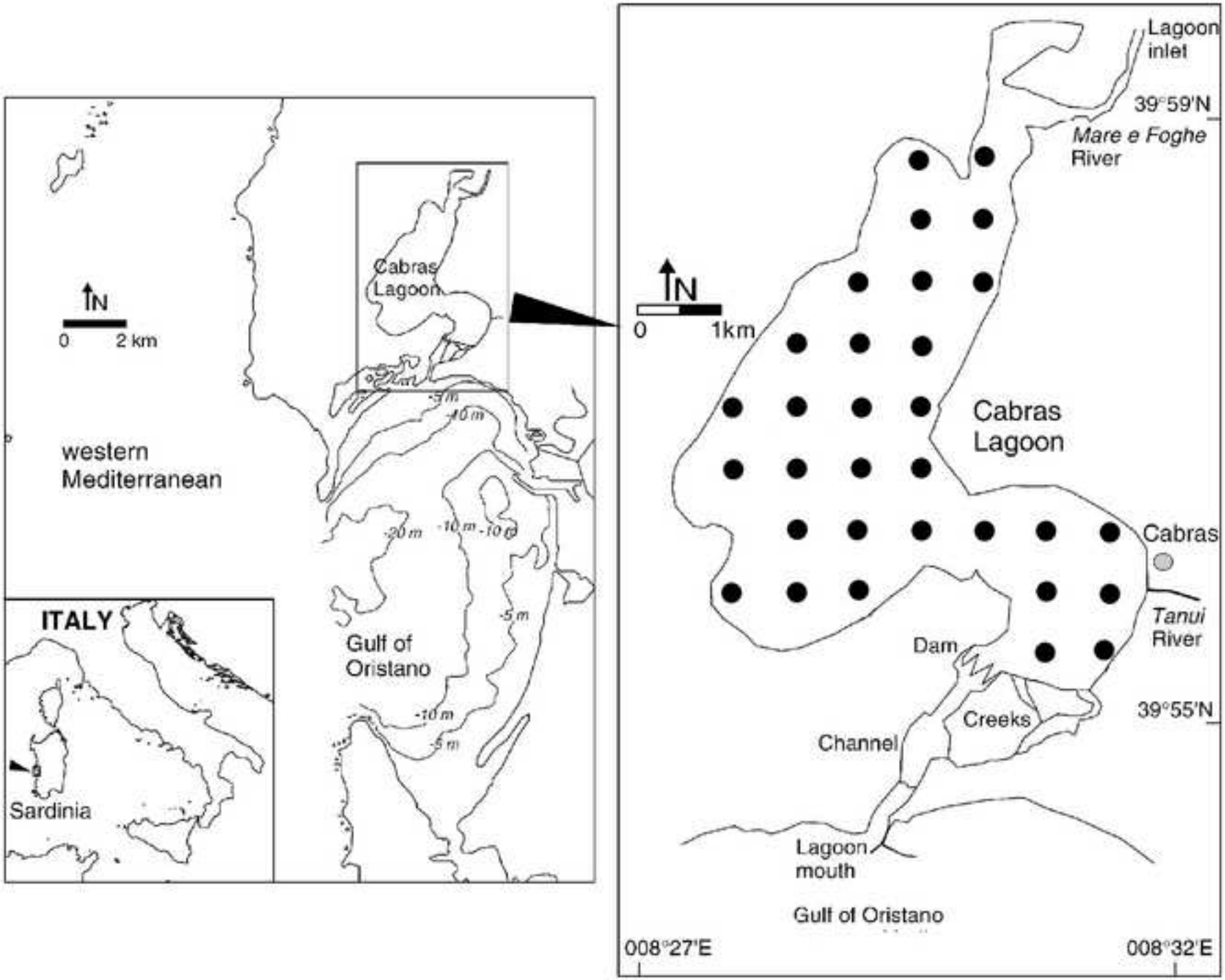
Lagoon inlet
39°59'N
Mare e Foghe River
N
0 2 km
Cabras Lagoon
western Mediterranean
-5 m
-10 m
-20 m
-10 m
-10 m
-5 m
ITALY
Sardinia
Gulf of Oristano
-10 m
-5 m
N
0 1km
Cabras Lagoon
Cabras
Tanui River
Dam
Creeks
39°55'N
Channel
Lagoon mouth
Gulf of Oristano
008°27'E
008°32'E

Figure 3

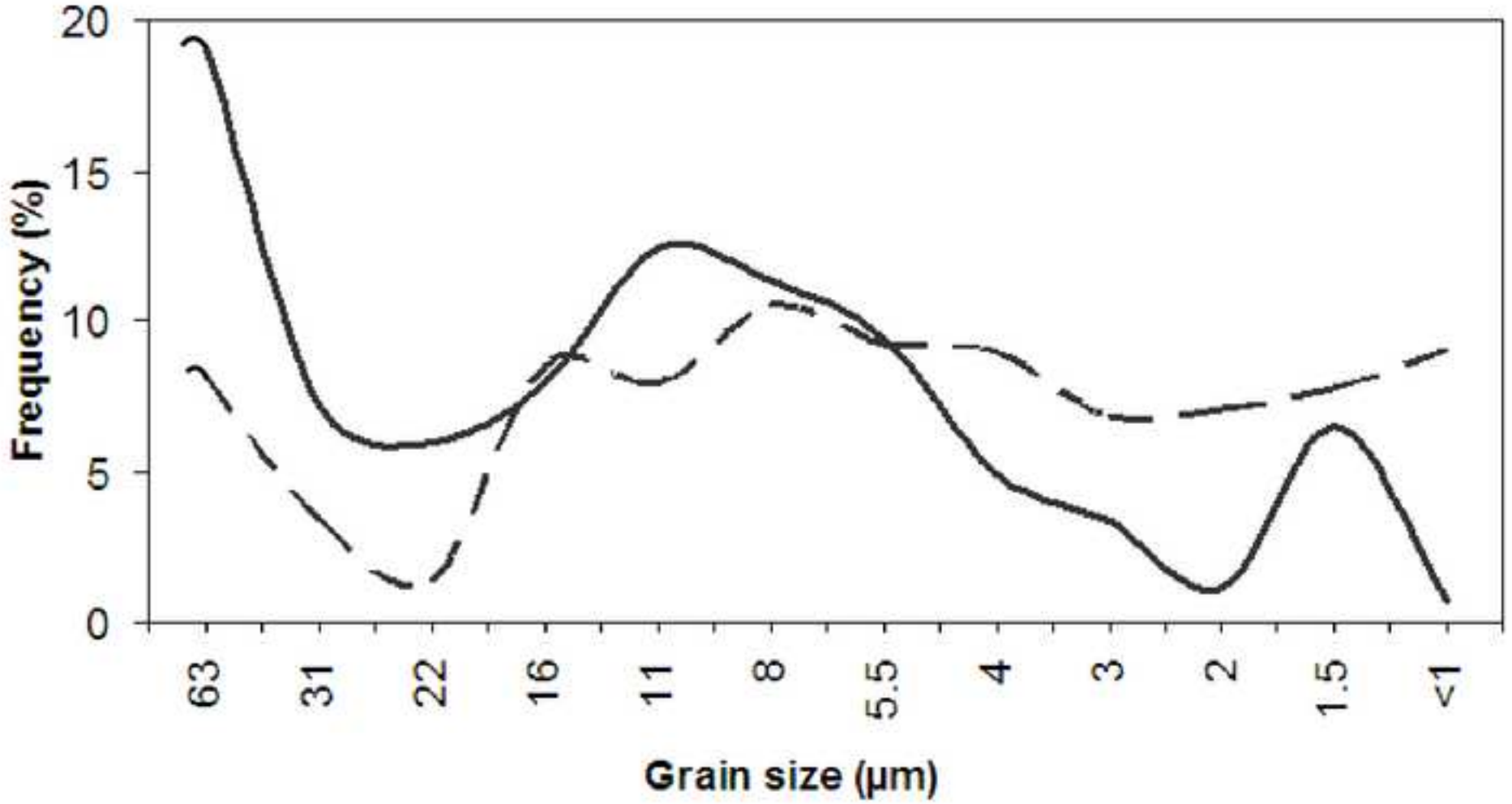

Figure 4

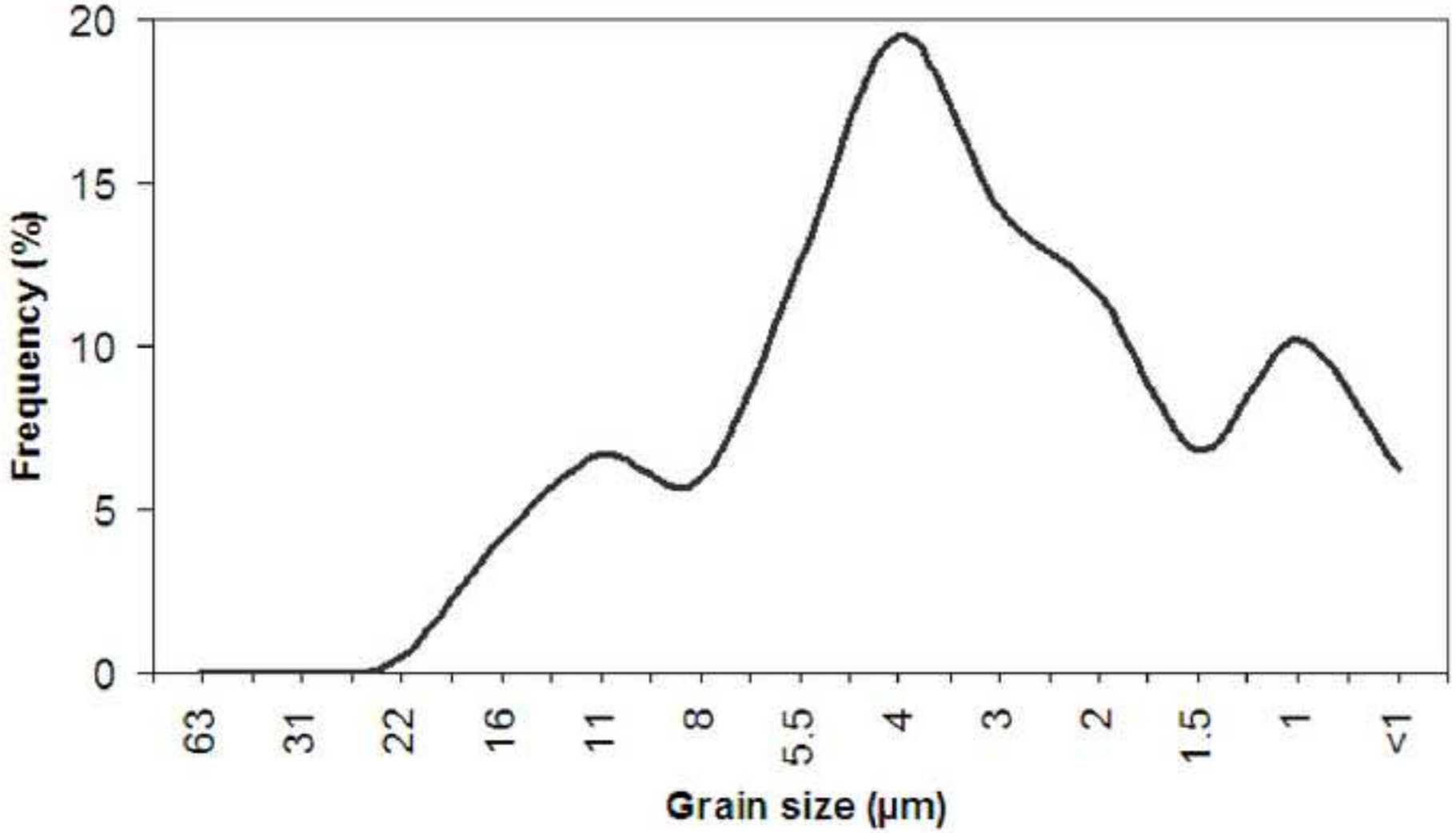

Figure 5

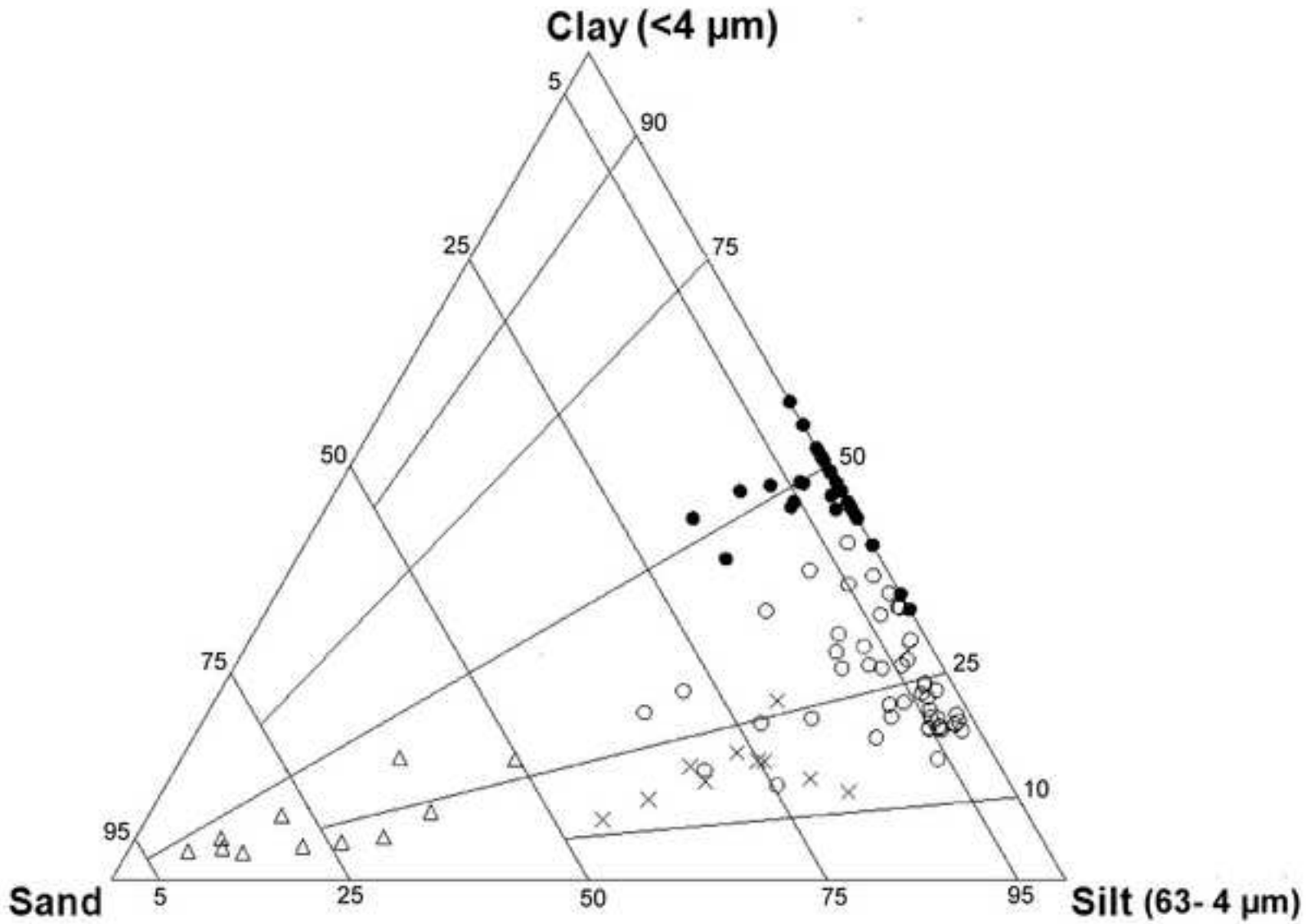

Figure 6

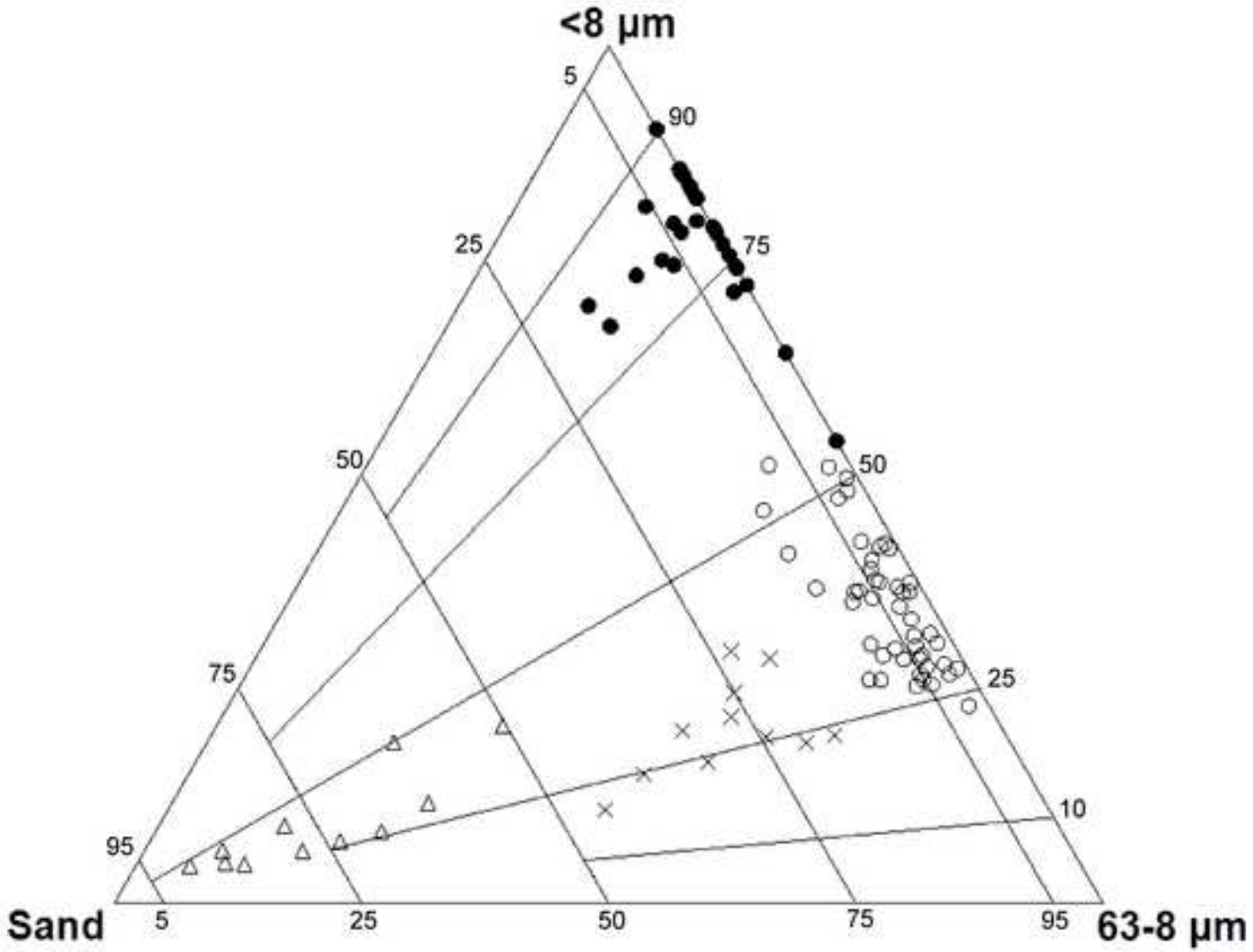

Figure 7

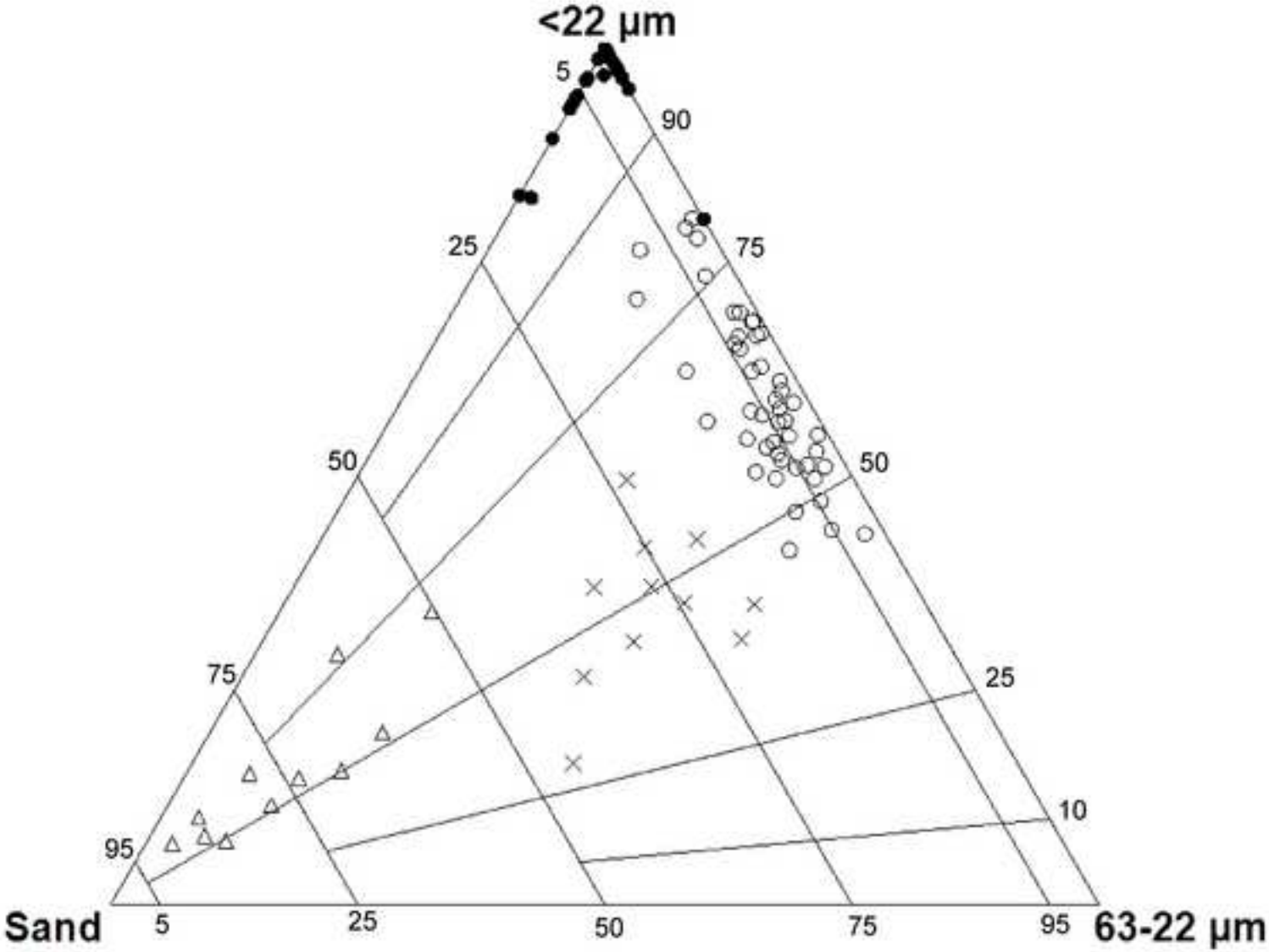

Figure 8

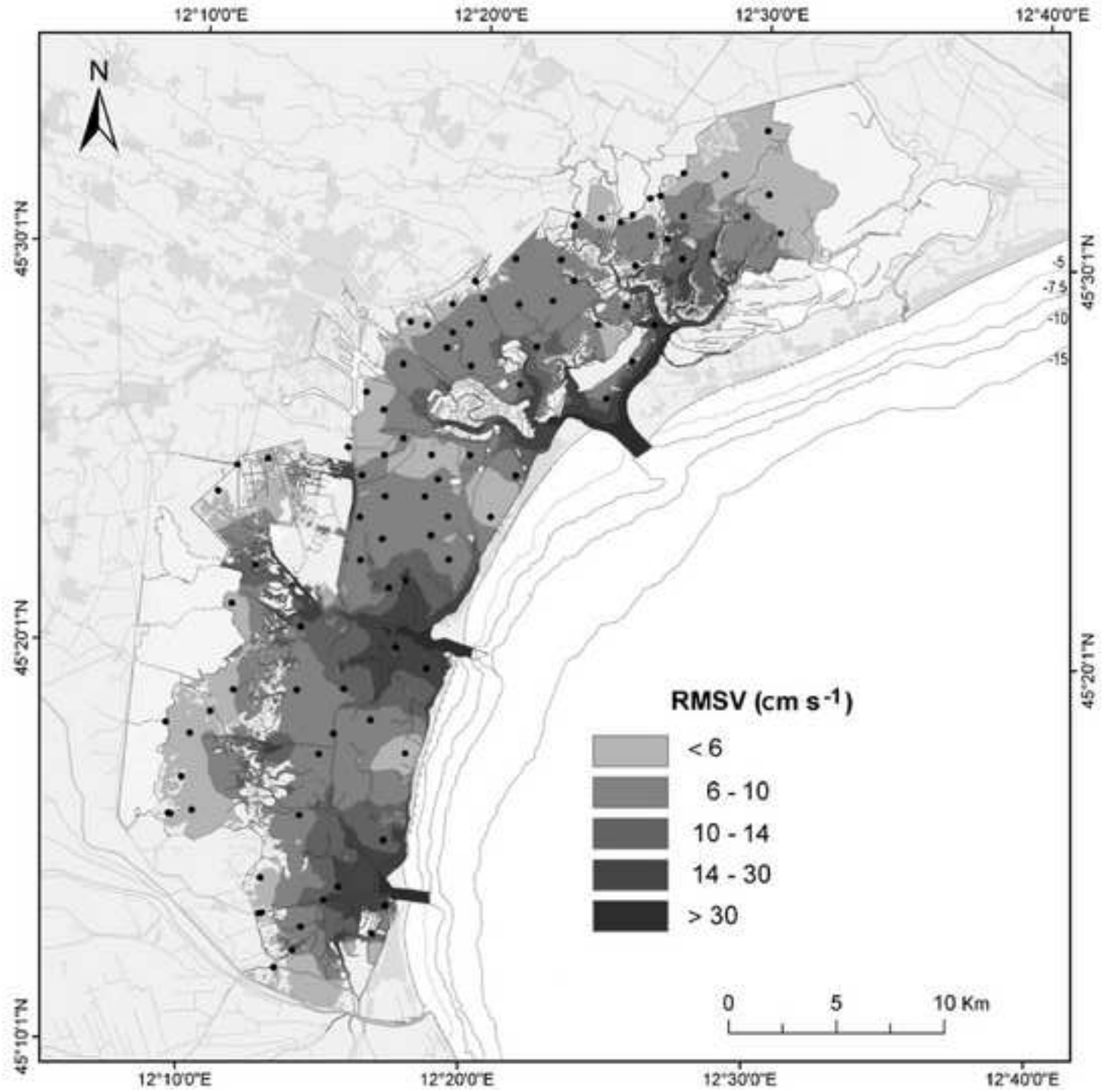
12°10'0"E
12°20'0"E
12°30'0"E
12°40'0"E
N
45°30'1"N
45°20'1"N
45°10'1"N
-5
-7.5
-10
-15
RMSV (cm s-1)
< 6
6 - 10
10 - 14
14 - 30
> 30
0
5
10 Km

Figure 9

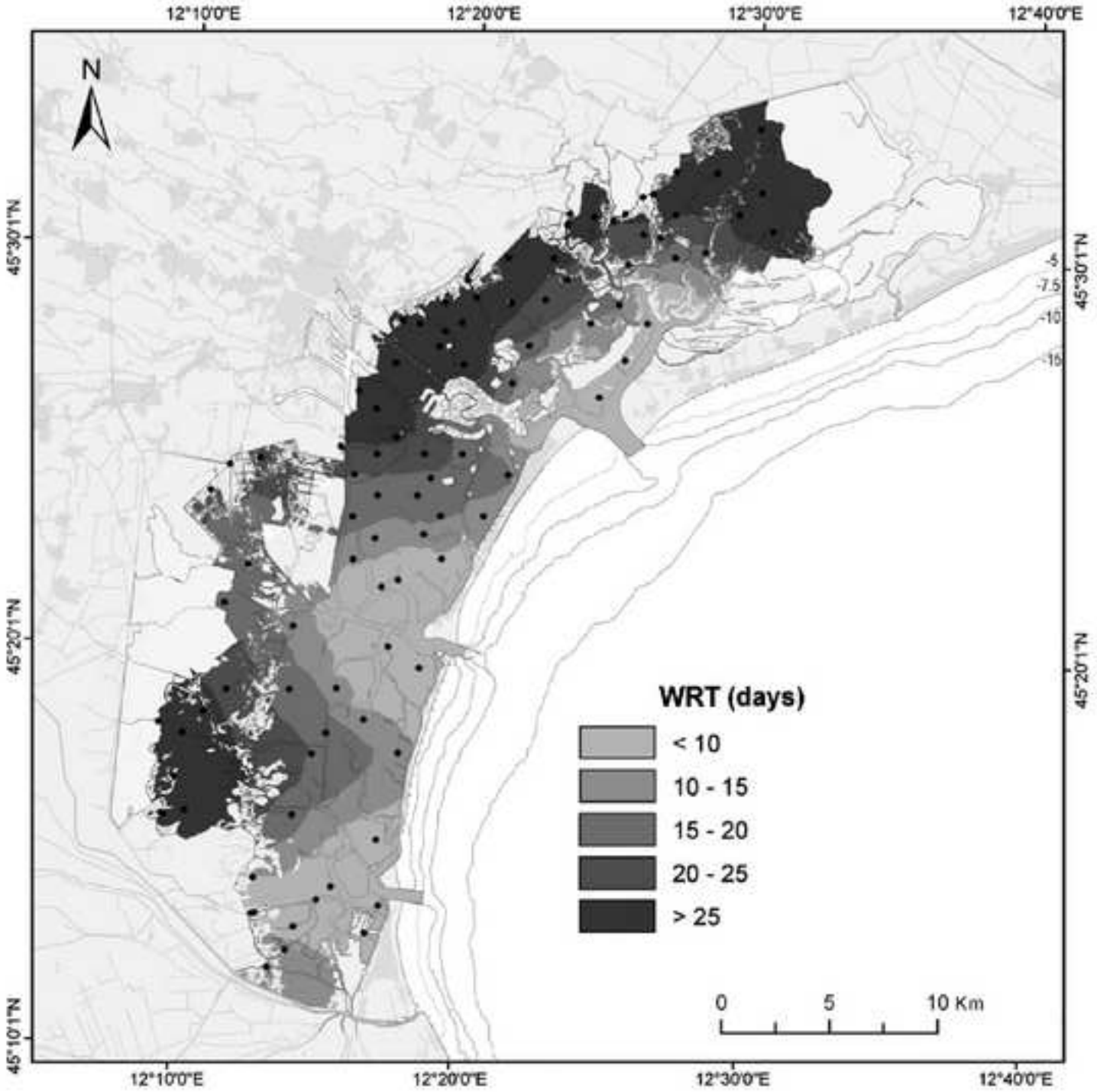
12°10'0"E
12°20'0"E
12°30'0"E
12°40'0"E
N
45°30'1"N
45°20'1"N
45°10'1"N
-5
-7.5
-10
-15
WRT (days)
< 10
10 - 15
15 - 20
20 - 25
> 25
0
5
10 Km

Figure 10

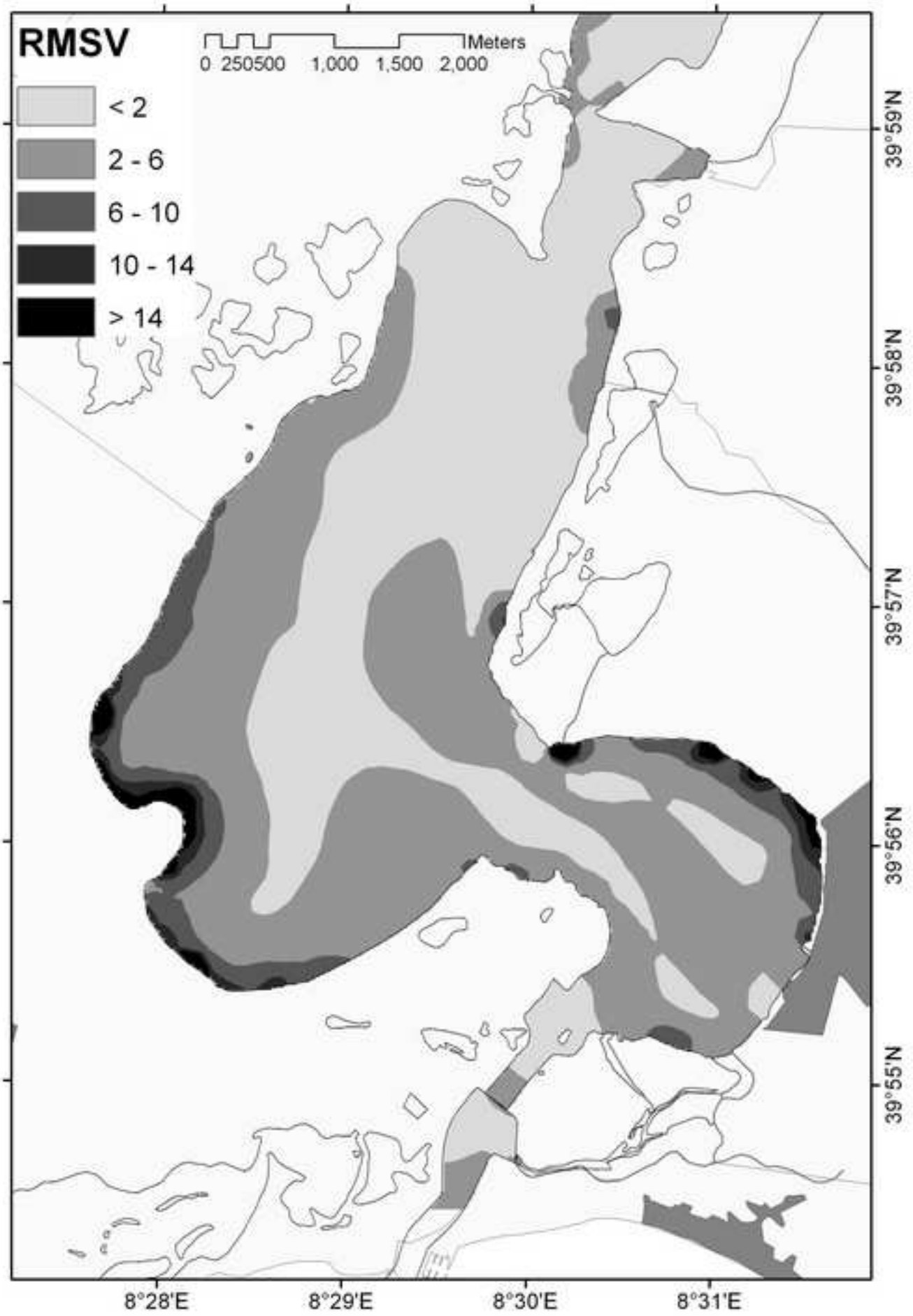
RMSV
0 250500 1,000 1,500 2,000
Meters
< 2
2 - 6
6 - 10
10 - 14
> 14
39°59'N
39°58'N
39°57'N
39°56'N
39°55'N
8°28'E
8°29'E
8°30'E
8°31'E

Figure 11

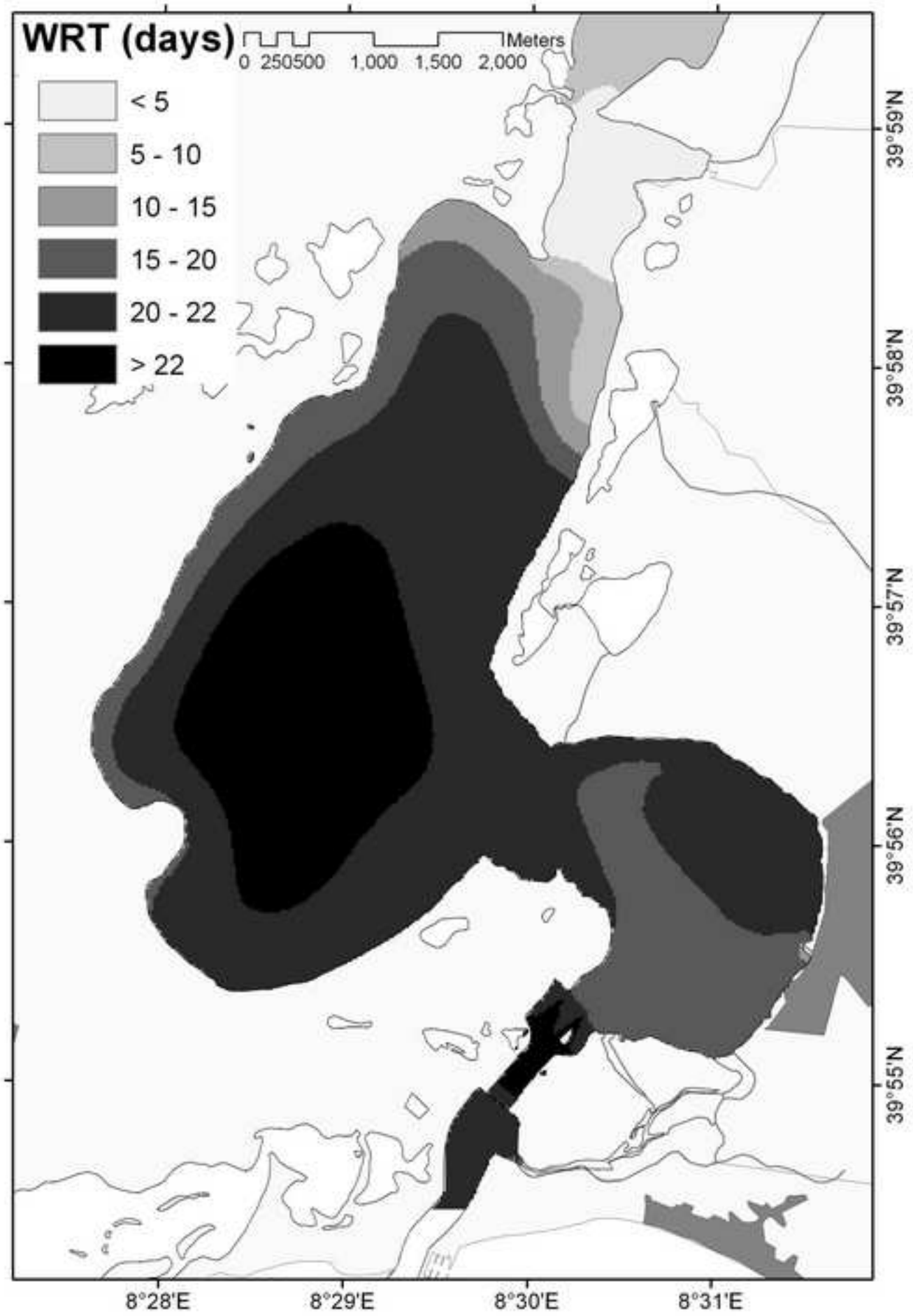
WRT (days)
Meters
0 250500 1,000 1,500 2,000
< 5
5 - 10
10 - 15
15 - 20
20 - 22
> 22
39°59'N
39°58'N
39°57'N
39°56'N
39°55'N
8°28'E
8°29'E
8°30'E
8°31'E

Figure 12

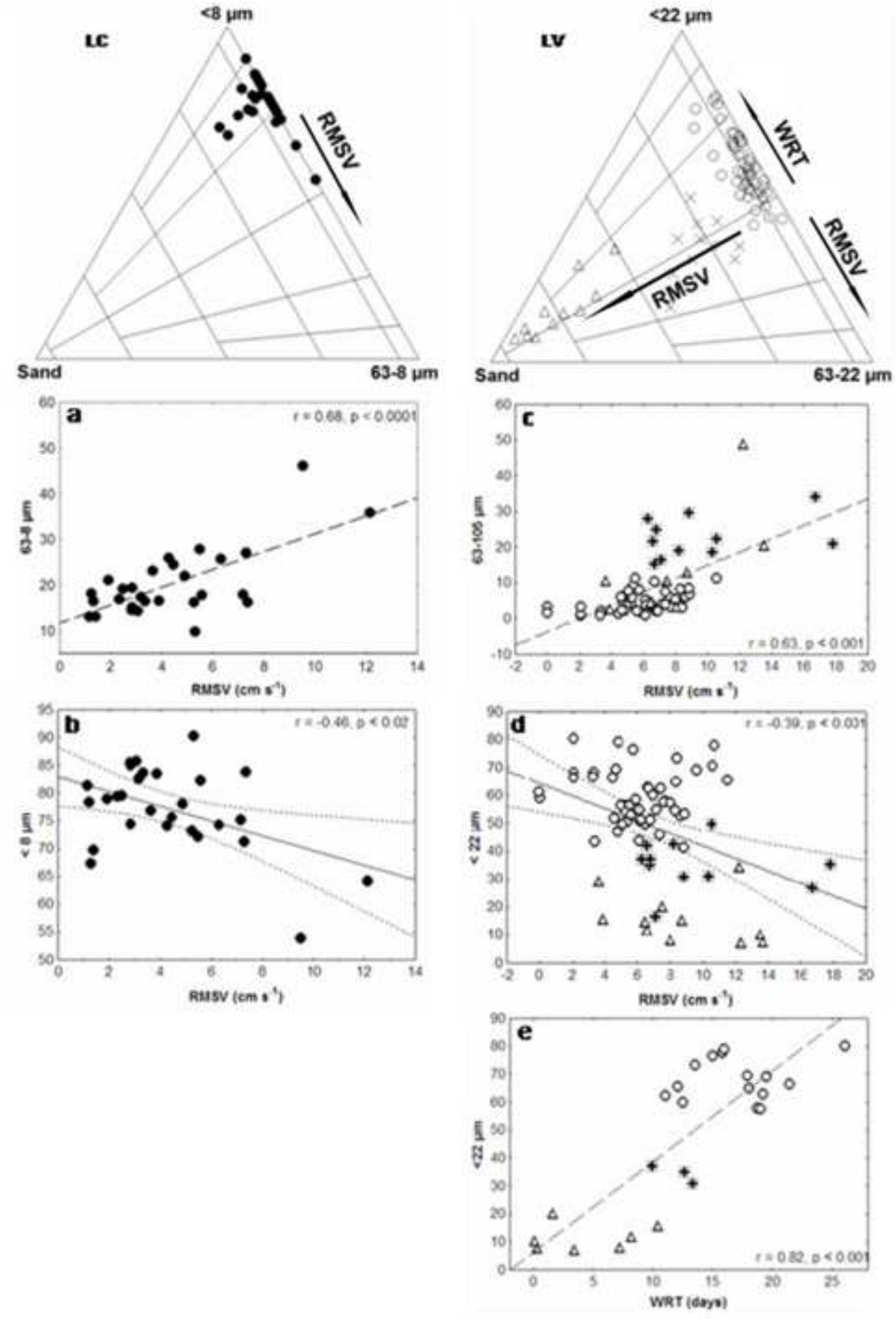
<8 µm
LC
RMSV
Sand
63-8 µm
<22 µm
LV
WRT
RMSV
RMSV
Sand
63-22 µm
a
r = 0.68, p < 0.0001
63-8 µm
RMSV (cm s-1)
c
r = 0.63, p < 0.001
63-105 µm
RMSV (cm s-1)
b
r = -0.46, p < 0.02
< 8 µm
RMSV (cm s-1)
d
r = -0.39, p < 0.001
< 22 µm
RMSV (cm s-1)
e
r = 0.82, p < 0.001
<22 µm
WRT (days)